

# Causal Mediation Analysis with a Three-Dimensional Image Mediator

Minghao Chen and Yingchun Zhou\*

Key Laboratory of Advanced Theory and Application in Statistics and Data Science-MOE,  
Institute of Brain and Education Innovation, School of Statistics,  
East China Normal University 3663 North Zhongshan Road, Shanghai, 200062, P.R. China

## Abstract

Causal mediation analysis is increasingly abundant in biology, psychology, and epidemiology studies, etc. In particular, with the advent of the big data era, the issue of high-dimensional mediators is becoming more prevalent. In neuroscience, with the widespread application of magnetic resonance technology in the field of brain imaging, studies on image being a mediator emerged. In this study, a novel causal mediation analysis method with a three-dimensional image mediator is proposed. We define the average casual effects under the potential outcome framework, explore several sufficient conditions for the valid identification, and develop techniques for estimation and inference. To verify the effectiveness of the proposed method, a series of simulations under various scenarios is performed. Finally, the proposed method is applied to a study on the causal effect of mother's delivery mode on child's IQ development. It is found that the white matter in certain regions of the frontal-parietal and brainstem-cerebellum areas has mediating effects.

**Keywords:** Causal inference; Mediation analysis; Structural equation model; Three-dimensional image data.

## 1 INTRODUCTION

Decoding the cognitive functions of the brain is currently one of the most challenging scientific problems in the world (Casey et al., 2005; Giedd and Rapoport, 2010). Recently, there has been an increasing interest in augmenting this study with mediation analysis that determines whether the effect of an external exposure on the cognitive or behavioral outcome is mediated by some latent intermediate variables, and estimates these indirect effects (Caffo et al., 2008; Lindquist,

---

\*Co-corresponding Authors: Yingchun Zhou, *E-mail address:* yczhou@stat.ecnu.edu.cn

2012; Zhao and Luo, 2019; Zhao et al., 2021). This study presents a novel method that models the magnetic resonance imaging (MRI) data as a three-dimensional mediator to reveal the underlying causal mechanism.

Mediation analysis was early developed in the psychology literature (e.g., James and Brett, 1984; Baron and Kenny, 1986), which frequently investigates the influences of the treatment on the mediator, the mediator on the outcome, and the treatment on the outcome via structural equation models (SEMs), with the model coefficients interpreted as direct and indirect effects. Later on, researches started to discuss the causality of mediation, that is, establishing the identifiability assumptions for the causal parameters of interest and constructing models to estimate or test the mediation effect simultaneously (e.g., Robins and Greenland, 1992; Pearl, 2001; Rubin, 2004; Albert, 2008; Imai et al., 2010b,a; VanderWeele, 2015). Causal mediation analysis has been widely used in many scientific areas, and a series of practical frameworks have been developed for different application scenarios. For example, VanderWeele and Vansteelandt (2014) and Daniel et al. (2015) considered the case of multiple intermediary variables. Lindquist (2012) and Zhao and Luo (2019) discussed longitudinal or functional mediators. Furthermore, with the advent of big data era, high-dimensional mediators are becoming more common in causal mediation analysis, and have been studied recently (e.g., Derkach et al., 2019; Dai et al., 2020; Zhou et al., 2020; Liu et al., 2022; Zhang et al., 2021; Guo et al., 2022). In particular, the widespread application of MRI in the fields of psychology and biology appeals to establishing a framework of image causal mediation analysis (ICMA). However, studies considering image mediators in causal inference are rare.

To assess image mediation, we combine the potential outcome framework of Rubin (1974) with linear image structural equation models (LISEMs), and then show that under certain assumptions, it is possible to obtain a valid estimate of the average causal effects of the mediator from the parameters of the LISEMs. Furthermore, in order to determine whether an image has a mediation effect and which loci of the image are transmitting this effect, a test procedure is provided. Although some researchers have considered different strategies for the identification of direct and indirect effects in the cases when interactions and nonlinearities are present (e.g., Avin et al., 2005; Petersen et al., 2006; Imai et al., 2010a; VanderWeele, 2015; Miles et al., 2020), in this paper we are only concerned with the type of additive models that are commonly used in the social sciences and leave other issues for future work.

Additionally, similar to the studies involving high-dimensional variables in causal inference (e.g., Luo et al., 2017; Zhang et al., 2018, 2020), regularization for the image coefficient of the second model in the LISEMs are required. While image belongs to high-dimensional data, it is often highly structured, which makes the common dimension reduction methods such as the LASSO method (Tibshirani, 1996) less effective (e.g., Zhou and Li, 2014; Wang et al., 2017). Different from two-dimensional images which are considered as matrices, the three-dimensional images in this study are treated as tensors. Thus the method proposed in a recent work considering the LISEMs with

two-dimensional image variables (Yu et al., 2022) is unsuitable for this study, since the tensor nuclear norm regularization approach is computationally intractable (Friedland and Lim, 2018). To solve the tensor estimation problem in the second model of the LISEMs, the image coefficient is regularized with low Tucker rank (Tucker, 1966). Other methods (e.g., Li, 2011; Zhou et al., 2013) that are applicable to estimating tensors of various structures can also be used in the proposed ICMA method.

This paper is structured as follows. In Section 2, the proposed ICMA method is described, including definition of average casual effects, establishment of valid identifiability assumptions, and description of procedures for estimating parameters and making inference. In Section 3, a series of simulation studies is conducted to verify the performance of the proposed method. In Section 4, the ICMA method is applied to the real data, and some enlightening results are obtained.

## 2 METHODOLOGY

In this section, we integrate the potential outcome framework of Rubin (1974) with SEMs to construct a framework of image causal mediation analysis. The notations are as follows. Let  $\mathbb{Z} = \{Z_j\}_{j=1, \dots, J}$  denote the set of all pre-treatment confounding variables. Throughout this article, assume  $Z_j$ 's are all scalars and fully observed with  $J \ll n$ , where  $n$  is the sample size. Let  $X$  be the binary treatment variable (0 or 1 corresponding to two treatments). Let  $Y$  be the continuous outcome. Denote  $\mathbf{M}$  as the three-dimensional image mediator. In practice, this imaging data is often represented in the form of a three-dimensional tensor. Assume that the tensors in this study are of type  $N_1 \times N_2 \times N_3$ , and  $N = \prod_{d=1}^3 N_d$  may be much larger than  $n$ . Additionally, let  $\mathcal{Z}$ ,  $\mathcal{M}$  and  $\mathcal{Y}$  denote the support of the distributions of  $\mathbb{Z}$ ,  $\mathbf{M}$  and  $Y$ , respectively.

### 2.1 Definition and Identification of the Causal Effects

In this section the causal effects of interest are defined and the assumptions for identifiability are established. First, the stable unit treatment value assumption (SUTVA; Rubin, 1980) that there is no interference between individuals is assumed. The statement below is analogous to that in Angrist et al. (1996).

**Assumption 1** (Stable Unit Treatment Value Assumption).

For each unit  $i$  :

- (a) If  $x_i = x'_i$ , then  $\mathbf{M}_i(x_1, \dots, x_n) = \mathbf{M}_i(x'_1, \dots, x'_n)$ ,  
 $Y_i(\{x_l\}_{l=1, \dots, n}, \{\mathbf{M}_l(\{x_l\}_{l=1, \dots, n})\}_{l=1, \dots, n}) = Y_i(\{x'_l\}_{l=1, \dots, n}, \{\mathbf{M}_l(\{x'_l\}_{l=1, \dots, n})\}_{l=1, \dots, n})$ ,  
and  $Y_i(\{x_l\}_{l=1, \dots, n}, \{\mathbf{M}_l(\{1 - x_l\}_{l=1, \dots, n})\}_{l=1, \dots, n}) = Y_i(\{x'_l\}_{l=1, \dots, n}, \{\mathbf{M}_l(\{1 - x'_l\}_{l=1, \dots, n})\}_{l=1, \dots, n})$ .
- (b) If  $x_i = x'_i$  and  $\mathbf{m}_i = \mathbf{m}'_i$ , then  $Y_i(\{x_l\}_{l=1, \dots, n}, \{\mathbf{m}_l\}_{l=1, \dots, n}) = Y_i(\{x'_l\}_{l=1, \dots, n}, \{\mathbf{m}'_l\}_{l=1, \dots, n})$ .

SUTVA implies that potential outcomes for each person are unrelated to the treatment given to

other individuals. Under SUTVA, let  $\mathbf{M}_i(x)$  denote the potential value of the mediator for unit  $i$  under the treatment status  $X_i = x$ ,  $Y_i(x, \mathbf{M}_i(x'))$  represent the potential outcome for unit  $i$  under  $X_i = x$  and  $\mathbf{M}_i(x')$ , and  $Y_i(x, \mathbf{m})$  be the potential outcome for unit  $i$  when  $X_i = x$  and  $\mathbf{M}_i = \mathbf{m}$ . Additionally, the observed variables can be written as  $\mathbf{M}_i = \mathbf{M}_i(X_i)$  and  $Y_i = Y_i(X_i, \mathbf{M}_i(X_i))$ .

Under SUTVA, the unit-level causal effects of  $X$  on  $\mathbf{M}$  and  $Y$ , respectively, for individual  $i$  ( $i \in \{1, \dots, n\}$ ), are given by the expressions

$$\mathbf{M}_i(1) - \mathbf{M}_i(0), \quad (1)$$

$$Y_i(1, \mathbf{M}_i(1)) - Y_i(0, \mathbf{M}_i(0)). \quad (2)$$

Then (2) can be decomposed as follows.

$$\begin{aligned} & Y_i(1, \mathbf{M}_i(1)) - Y_i(0, \mathbf{M}_i(0)) \\ &= \{Y_i(1, \mathbf{M}_i(0)) - Y_i(0, \mathbf{M}_i(0))\} + \{Y_i(1, \mathbf{M}_i(1)) - Y_i(1, \mathbf{M}_i(0))\} \\ &= \{Y_i(1, \mathbf{M}_i(1)) - Y_i(0, \mathbf{M}_i(1))\} + \{Y_i(0, \mathbf{M}_i(1)) - Y_i(0, \mathbf{M}_i(0))\}. \end{aligned} \quad (3)$$

In both decompositions, the first term represents a natural direct effect of  $X$  on  $Y$  of subject  $i$ , while the second represents a natural indirect effect (Pearl, 2001).

Averaging (3) over all subjects, one obtains

$$\begin{aligned} & E(Y(1, \mathbf{M}(1)) - Y(0, \mathbf{M}(0))) \\ &= E(Y(1, \mathbf{M}(0)) - Y(0, \mathbf{M}(0))) + E(Y(1, \mathbf{M}(1)) - Y(1, \mathbf{M}(0))) \\ &= E(Y(1, \mathbf{M}(1)) - Y(0, \mathbf{M}(1))) + E(Y(0, \mathbf{M}(1)) - Y(0, \mathbf{M}(0))). \end{aligned} \quad (4)$$

Then the causal effects of interest are defined as follows.

**Definition 1** (Average Total Effect).

$$\tau := E(Y(1, \mathbf{M}(1)) - Y(0, \mathbf{M}(0))). \quad (5)$$

**Definition 2** (Average Causal Direct Effect).

$$\gamma(x) := E(Y(1, \mathbf{M}(x))) - E(Y(0, \mathbf{M}(x))), \quad (6)$$

for  $x = 0, 1$ .

**Definition 3** (Average Causal Indirect Effect).

$$\delta(x) := E(Y(x, \mathbf{M}(1))) - E(Y(x, \mathbf{M}(0))), \quad (7)$$

for  $x = 0, 1$ .

In general, the average causal direct and indirect effects defined above are different from the average controlled effect of the treatment, that is,  $E(Y(x, \mathbf{m}) - Y(x', \mathbf{m}))$  for  $x \neq x'$  and all  $\mathbf{m} \in \mathcal{M}$ , and that of the mediator, that is,  $E(Y(x, \mathbf{m}) - Y(x, \mathbf{m}'))$  for  $x = 0, 1$  and  $\mathbf{m} \neq \mathbf{m}'$  (Pearl, 2001; Robins, 2003). Unlike the causal effects  $\gamma(x)$  and  $\delta(x)$ , the controlled effects are defined in terms of specific values of the mediator, rather than its potential values.

Since for individual  $i$  only one of  $\{\mathbf{M}_i(1), Y_i(1, \mathbf{M}_i(1))\}$  and  $\{\mathbf{M}_i(0), Y_i(0, \mathbf{M}_i(0))\}$  can be observed, the unit-level causal effects cannot be directly calculated. Nevertheless, it will be shown that the average causal effects defined above can be identified and validly estimated under certain assumptions.

**Assumption 2** (Sequential ignorability).

$$(a) \quad \{Y_i(x', \mathbf{m}), \mathbf{M}_i(x)\} \perp X_i \mid \mathbb{Z}_i = z,$$

$$(b) \quad Y_i(x', \mathbf{m}) \perp \mathbf{M}_i(x) \mid X_i = x, \mathbb{Z}_i = z$$

for  $x, x' = 0, 1$ , and all  $z \in \mathcal{Z}$ , where it is also assumed that  $0 < \Pr(X = x \mid \mathbb{Z}_i = z)$  and  $0 < \Pr(\mathbf{M}(x) = m \mid X = x, \mathbb{Z} = z)$  for  $x = 0, 1$ , and all  $z \in \mathcal{Z}$  and  $\mathbf{m} \in \mathcal{M}$ .

Assumption 2 is called the sequential ignorability assumption, which has been carefully described and compared with other strong assumptions when the intermediary variable is a one-dimensional variable in Imai et al. (2010b). In this study, this assumption is extended to the image mediator case. It is easy to show that  $\gamma(x)$  and  $\delta(x)$  are nonparametrically identified under Assumption 2. However, it is not easy to estimate them since estimating the conditional distribution of a tensor-valued random variable is difficult and the estimate often does not have a closed form expression, even if the entries of  $\mathbf{M}$  are independently normally distributed (Hoff, 2011). To this end, seeking sufficient conditions for validly estimating  $\tau$ ,  $\gamma(x)$  and  $\delta(x)$  is necessary.

**Assumption 3.** The observed variables of each individual  $i \in \{1, \dots, n\}$  follow the LISEMs, that is,

$$\mathbf{M}_i = \boldsymbol{\eta}_1 + X_i * \boldsymbol{\alpha} + \sum_{j=1}^J Z_{ij} * \boldsymbol{\Psi}_j + \boldsymbol{\varepsilon}_i, \quad (8)$$

$$Y_i = \eta_2 + X_i \gamma + \langle \mathbf{M}_i, \boldsymbol{\beta} \rangle + \sum_{j=1}^J Z_{ij} s_j + \epsilon_i, \quad (9)$$

where  $E(\boldsymbol{\varepsilon} \mid X = x, \mathbb{Z} = z) = \mathbf{0}$ ,  $E(\epsilon \mid X = x, \mathbf{M} = \mathbf{m}, \mathbb{Z} = z) = 0$ ,  $c * \mathbf{U} = \{cu_{p_1, p_2, p_3}\}_{d=1,2,3}^{1 \leq p_d \leq N_d}$  denotes the scalar multiplication between the scalar  $c$  and tensor  $\mathbf{U} = \{u_{p_1, p_2, p_3}\}_{d=1,2,3}^{1 \leq p_d \leq N_d}$ , and  $\langle \mathbf{U}, \mathbf{V} \rangle = \sum_{p_1, p_2, p_3} u_{p_1, p_2, p_3} v_{p_1, p_2, p_3}$  denotes the inner product between the tensors  $\mathbf{U} = \{u_{p_1, p_2, p_3}\}_{d=1,2,3}^{1 \leq p_d \leq N_d}$  and  $\mathbf{V} = \{v_{p_1, p_2, p_3}\}_{d=1,2,3}^{1 \leq p_d \leq N_d}$ .

Assumption 3 extends the linear structural equation models in Baron and Kenny (1986) to LISEMs by mainly replacing  $M_i$  with  $\mathbf{M}_i$ , and allows that the observed variables follow the LISEMs.

Under Assumptions 1-3, one can obtain a valid estimate of the average causal effects from the parameters of the LISEMs, which is presented in the following theorem.

**Theorem 1.** *If Assumptions 1, 2 and 3 hold, then the causal effects  $\tau$ ,  $\gamma(x)$  and  $\delta(x)$  can be expressed as*

$$\begin{aligned}\tau &= \gamma + \langle \boldsymbol{\beta}, \boldsymbol{\alpha} \rangle, \\ \gamma(x) &= \gamma, \\ \delta(x) &= \langle \boldsymbol{\beta}, \boldsymbol{\alpha} \rangle,\end{aligned}$$

for  $x = 0, 1$ .

See Appendix A for a proof. Theorem 1 implies that there is no interaction between the treatment and the mediator, that is,  $\gamma(0) = \gamma(1)$  and  $\delta(0) = \delta(1)$ .

Alternatively, inspired by the relationship between the average controlled causal effects and the average natural causal effects (e.g., Zheng and Zhou, 2015), we find some conditions that are weaker than Assumptions 2 and 3, but still sufficient to identify  $\tau$ ,  $\gamma(x)$  and  $\delta(x)$ . These conditions are summarized in Assumption 4.

**Assumption 4.**

- (a)  $E\{\mathbf{M}(x) \mid X = x, \mathbb{Z} = z\} = E\{\mathbf{M}(x) \mid \mathbb{Z} = z\},$   
 $E\{Y(x, \mathbf{M}(x)) \mid X = x, \mathbf{M}(x) = m, \mathbb{Z} = z\} = E\{Y(x, \mathbf{M}(x)) \mid \mathbf{M}(x) = m, \mathbb{Z} = z\},$
- (b)  $E\{Y(x, \mathbf{m}) \mid \mathbf{M}(x') = \mathbf{m}, \mathbb{Z} = z\} = E\{Y(x, \mathbf{m}) \mid \mathbb{Z} = z\},$
- (c)  $0 < Pr(X = x \mid \mathbb{Z}_i = z)$  and  $0 < p(\mathbf{M}(x) = m \mid \mathbb{Z} = z),$
- (d)  $E\{\mathbf{M}(x) \mid \mathbb{Z} = z\} = \boldsymbol{\eta}_1^{(c)} + x * \boldsymbol{\alpha}^{(c)} + \sum_{j=1}^J z_j * \boldsymbol{\Psi}_j^{(c)},$   
 $E\{Y(x, \mathbf{m}) \mid \mathbb{Z} = z\} = \eta_2^{(c)} + x\gamma^{(c)} + \langle \mathbf{m}, \boldsymbol{\beta}^{(c)} \rangle + \sum_{j=1}^J z_j s_j^{(c)}$

for  $x = 0, 1$ , and all  $z \in \mathcal{Z}$  and  $\mathbf{m} \in \mathcal{M}$ .

Under Assumptions 1 and 4 (d), the average controlled direct effect of the treatment is defined as  $E(Y(1, \mathbf{m}) - Y(0, \mathbf{m})) = \gamma^{(c)}$  and the average controlled effect of  $X$  on  $\mathbf{M}$ , and  $\mathbf{M}$  on  $Y$  at level  $\mathbf{m}$  versus  $\mathbf{m}'$  can be written as  $E(\mathbf{M}(1) - \mathbf{M}(0)) = \boldsymbol{\alpha}^{(c)}$ ,  $E(Y(x, \mathbf{m}) - Y(x, \mathbf{m}')) = \langle \mathbf{m} - \mathbf{m}', \boldsymbol{\beta}^{(c)} \rangle$ , respectively. Further, under Assumptions 1 and 4 (a)-(c), the parameters  $\boldsymbol{\alpha}^{(c)} = \boldsymbol{\alpha}$ ,  $\gamma^{(c)} = \gamma$  and  $\boldsymbol{\beta}^{(c)} = \boldsymbol{\beta}$ , which in general do not hold (Sobel, 2008; Lindquist, 2012). Then the average controlled causal effects can be expressed by the parameters of the LISEMs. It follows that  $\tau$ ,  $\gamma(x)$  and  $\delta(x)$  can be validly identified under Assumptions 1 and 4. These results are summarized in Theorem 2.

**Theorem 2.** *Under Assumptions 1 and 4,*

$$\begin{aligned}
\boldsymbol{\alpha}^{(c)} &= \boldsymbol{\alpha}, \quad \gamma^{(c)} = \gamma, \quad \boldsymbol{\beta}^{(c)} = \boldsymbol{\beta}, \quad \text{and} \\
E(\mathbf{M}(1) - \mathbf{M}(0)) &= \boldsymbol{\alpha}, \\
E(Y(1, \mathbf{m}) - Y(0, \mathbf{m})) &= \gamma, \\
E(Y(x, \mathbf{m}) - Y(x, \mathbf{m}')) &= \langle \mathbf{m} - \mathbf{m}', \boldsymbol{\beta} \rangle, \\
\tau &= \gamma + \langle \boldsymbol{\beta}, \boldsymbol{\alpha} \rangle, \quad \gamma(x) = \gamma, \quad \delta(x) = \langle \boldsymbol{\beta}, \boldsymbol{\alpha} \rangle,
\end{aligned}$$

for  $x = 0, 1$ , and all  $\mathbf{m} \in \mathcal{M}$ .

See Appendix A for the proof of Theorem 2, and the proof that Assumption 4 is weaker than Assumption 2 and 3.

## 2.2 Estimation and Inference

In this section an approach for estimating the causal parameters of interest in the LISEMs is described. Additionally, a procedure for testing the causal parameters based on the resampling techniques is provided.

### 2.2.1 Estimation

The LISEMs considered in this study are composed of two types of linear regression models. One consists of an image response and some scalar predictors, while the other consists of a scalar response, an image predictor, and some other scalar predictors. Since the second one is essentially a special high-dimensional linear model, it is assumed that the Tucker rank of the coefficient tensor  $\boldsymbol{\beta}$  is low so as to obtain a valid estimate, as well as to enhance power of the subsequent tests. Note that the proposed method is flexible, so other regularization methods that fit image data may also be used. Meanwhile, for further statistical inference, not penalizing other coefficient parameters leaves their estimators unbiased, and there is no need for conducting any of the debiased or decorrelated procedures (e.g., Zhang and Zhang, 2014; Van de Geer et al., 2014). Our estimation strategy is as follows.

For simplicity, the intercept terms is suppressed in the LISEMs,

$$\mathbf{M}_i = X_i * \boldsymbol{\alpha} + \sum_{j=1}^J Z_{ij} * \boldsymbol{\Psi}_j + \boldsymbol{\varepsilon}_i, \quad (10)$$

$$Y_i = X_i \gamma + \langle \mathbf{M}_i, \boldsymbol{\beta} \rangle + \sum_{j=1}^J Z_{ij} s_j + \epsilon_i. \quad (11)$$

First, an unbiased estimate of  $\Delta = (\alpha, \Psi_1, \dots, \Psi_J)$  can be obtained via the least square method based on (10), that is,

$$\begin{aligned}\hat{\Delta} &= \arg \min_{\alpha, \Psi_j \in \mathbb{R}^{N_1 \times N_2 \times N_3}} \sum_{i=1}^n \| \mathbf{M}_i - X_i * \alpha - Z_{ij} * \Psi_j \|_F^2 \\ &= \arg \min_{\alpha, \Psi_j \in \mathbb{R}^{N_1 \times N_2 \times N_3}} \| M - A_{X,Z} \Delta \|_2^2,\end{aligned}$$

where  $\|U\|_F^2 = \sum_{p_1, p_2, p_3} u_{p_1, p_2, p_3}^2$  denotes the Frobenius norm,  $M = (\text{vec}(\mathbf{M}_1)^T, \dots, \text{vec}(\mathbf{M}_n)^T)^T$ ,  $\alpha = \text{vec}(\alpha)$ , and  $\text{vec}(U) = (u_{1,1,1}, u_{2,1,1}, \dots, u_{N_1,1,1}, u_{1,2,1}, \dots, u_{N_1,2,1}, \dots, u_{N_1, N_2, N_3})^T$ . Additionally,  $A_{X,Z} = (A_X, A_{Z_1}, \dots, A_{Z_J})$ ,  $A_X = (X_1 I_N, \dots, X_n I_N)^T$ ,  $A_{Z_j} = (Z_{1j} I_N, \dots, Z_{nj} I_N)^T$ .

By substituting (10) into (11), one obtains that

$$Y_i = X_i \theta_0 + \sum_{j=1}^J Z_{ij} \theta_j + \xi_i, \quad (12)$$

where  $\theta_0 = \gamma + \langle \beta, \alpha \rangle$ ,  $\theta_j = s_j + \langle \beta, \Psi_j \rangle$ ,  $\xi_i = \langle \beta, \epsilon_i \rangle + \epsilon_i$ , and  $E(\xi \mid X = x) = 0$ .

Next, an estimate of  $\theta = (\theta_0, \dots, \theta_J)^T$  via the ordinary least square method based on (12) is as follows.

$$\begin{aligned}\hat{\theta} &= \arg \min_{\theta \in \mathbb{R}^{J+1}} \sum_{i=1}^n (Y_i - X_i \theta_0 - Z_{ij} \theta_j)^2 \\ &= \arg \min_{\theta \in \mathbb{R}^{J+1}} \| Y - B_{X,Z} \theta \|_2^2,\end{aligned}$$

where  $Y = (Y_1, \dots, Y_n)^T$ ,  $B_{X,Z} = (X, Z_1, \dots, Z_J)$ ,  $X = (X_1, \dots, X_n)^T$  and  $Z_j = (Z_{1j}, \dots, Z_{nj})^T$ .

In the following, it is shown that  $\beta$  in equation (11) can also be estimated by (13).

**Proposition 1.** Suppose  $\hat{\Delta} = (\hat{\alpha}, \hat{\Psi}_1, \dots, \hat{\Psi}_J)$  is the ordinary least square estimator of  $\Delta = (\alpha, \Psi_1, \dots, \Psi_J)$  of equation (10), and  $\hat{\theta}$  is the ordinary least square estimator of  $\theta$  of equation (12), then equation (11) can be rewritten as

$$\hat{\omega} = A_{\hat{\epsilon}} \beta + \hat{\epsilon}, \quad (13)$$

where  $\hat{\omega} = Y - B_{X,Z} \hat{\theta}$ ,  $\beta = \text{vec}(\beta)$ ,  $\hat{\epsilon} = \Lambda \epsilon$ , and  $A_{\hat{\epsilon}} = (\hat{\epsilon}_1, \dots, \hat{\epsilon}_n)^T$ ,  $\hat{\epsilon}_i = \text{vec}(\hat{\epsilon}_i)$ ,  $\hat{\epsilon}_i = \mathbf{M}_i - X_i * \hat{\alpha} - \sum_{j=1}^J Z_{ij} * \hat{\Psi}_j$ ,  $\Lambda = (I - B_{X,Z}^T (B_{X,Z}^T B_{X,Z})^{-1} B_{X,Z})$ .

See Appendix B for the proof of Proposition 1.

Estimating  $\beta$  based on equation (13) is a classical problem in statistics. Specifically, inspired by recent work (e.g., ?Ahmed et al., 2020; Han et al., 2022; Luo and Zhang, 2021), assuming the parameter  $\beta$  to have a low Tucker rank, we use the Tucker decomposition to solve the tensor



estimation problem. An estimate of  $\beta$  based on (13) is as follows.

$$\hat{\beta} = \arg \min_{\beta \in \mathcal{R}^{p_1 \times p_2 \times p_3}} \frac{1}{2} \|\hat{\omega} - A_{\hat{\varepsilon}} \beta\|_2^2, \quad \text{subject to} \quad \text{Tucker-rank}(\beta) = \mathbf{r}. \quad (14)$$

However, the optimization problem in (14) is generally non-convex and NP-hard. A large body of literature solve this problem by two-stage procedures: one first obtains a warm initialization of  $\beta$  and then runs local algorithms to refine the estimate. Among them, [Luo and Zhang \(2021\)](#) proposes a Riemannian Gauss Newton (RGN) method with fast implementations. In the RGN method, let  $A_{\hat{\varepsilon}} \beta = \mathcal{A}_{\hat{\varepsilon}}(\beta)$ , and if  $\mathcal{A}_{\hat{\varepsilon}}$  satisfies the tensor restricted isometry property (TRIP, [Rauhut et al., 2017](#)) at rank  $\mathbf{r}$  with high probability and the initialization is obtained by T-HOSVD ([De Lathauwer et al., 2000](#)), then the estimate  $\hat{\beta}$  achieves the minimax rate-optimal estimation error ([Luo and Zhang, 2021](#)). Due to these benefits, in this study  $\beta$  is estimated by solving the optimization problem in (14) via the RGN method.

Finally, an estimate of  $\gamma$  can be given by

$$\hat{\gamma} = \hat{\theta}_0 - \langle \hat{\alpha}, \hat{\beta} \rangle. \quad (15)$$

## 2.2.2 Inference

Another central question of mediation analysis is to determine whether  $\mathbf{M}$  acts as an intermediary to transmit the effect of  $X$  on  $Y$ , and which loci in  $\mathbf{M}$  transmit that effect. Analogous to the univariate setting ([Sobel, 1982](#); [Baron and Kenny, 1986](#); [Lindquist, 2012](#)), these can be done by testing whether  $\langle \alpha, \beta \rangle$  differs from 0, and whether  $\alpha \circ \beta$  (the Hadamard product ([Kressner and Perisa, 2017](#)) for  $\alpha$  and  $\beta$ ) differs from  $\mathbf{0}$ . Since the exact distribution of  $\alpha \circ \beta$  is unknown, bootstrap methods are used to perform inference. The procedure for obtaining the bootstrap distribution of  $\alpha \circ \beta$  is as follows.

**Step 1.** Estimating the parameters of interest based on the LISEMs and the original data via the strategy proposed in Section 2.2.1.

**Step 2.** Independently generating a bootstrap sample  $(\mathbb{Z}_i, X_i, \mathbf{M}_i^\dagger, Y_i^\dagger)$ ,  $i \in \{1, \dots, n\}$  based on LISEMs, that is,

$$\begin{aligned} \mathbf{M}_i^\dagger &= \hat{\eta}_1 + X_i * \hat{\alpha} + \sum_{j=1}^J Z_{ij} * \hat{\Psi}_j + v_i^\dagger \hat{\varepsilon}_i, \\ Y_i^\dagger &= \hat{\eta}_2 + X_i \hat{\delta} + \langle \hat{\beta}, \mathbf{M}_i^\dagger \rangle + \sum_{j=1}^J Z_{ij} \hat{s}_j + v_i^\dagger \hat{\varepsilon}_i, \end{aligned}$$

where  $\hat{\varepsilon}_i = \mathbf{M}_i - \hat{\eta}_1 - X_i * \hat{\alpha} - \sum_{j=1}^J Z_{ij} * \hat{\Psi}_j$ ,  $\hat{\varepsilon}_i = Y_i - \hat{\eta}_2 - X_i \hat{\delta} - \langle \hat{\beta}, \mathbf{M}_i \rangle - \sum_{j=1}^J Z_{ij} \hat{s}_j$ ,  $v_i^\dagger$  are

independent and identically distributed and  $Pr(v_i^\dagger = 1) = Pr(v_i^\dagger = -1) = \frac{1}{2}$ .

**Step 3.** Estimating the parameters of interest again based on the LISEMs and the bootstrap samples generated in Step 2.

**Step 4.** Repeat the procedure outlined in Steps 2 and 3 for a prespecified number of times (e.g., 500 times). These replications are used to compute the bootstrap distribution of  $\alpha \circ \beta$ .

One can also compute percentile confidence ‘zone’ for  $\alpha \circ \beta$  via the bootstrap distribution (Efron and Tibshirani, 1994).

As we are interested in testing whether  $\alpha \circ \beta$  differs from  $\mathbf{0}$  at each locus, it is necessary to adjust the p-values for multiple comparisons. Throughout the article, the Benjamini–Hochberg procedure (Benjamini and Hochberg, 1995) is used to control the false discovery rate (FDR).

### 3 SIMULATION

In this section, simulation studies are conducted and the performance of the ICMA method is shown in various scenarios.

The simulation data  $(Z_i, X_i, \mathbf{M}_i, Y_i)$ ,  $i = 1, \dots, n$ ,  $n = 100$ ,  $N_1 = N_2 = N_3 = 8$  are generated based on five causal diagrams (five scenarios) which commonly occur in causal mediation analysis. The first three scenarios do not have mediation effect, that is, the treatment has no effect on the mediator or the mediator has no effect on the outcome. The remaining two scenarios are set to have a mediation effect. The specific settings of the five scenarios are summarized in Table 1.

Table 1: The summary of simulation settings.

Scenario	$X$	$\mathbf{M}$	$Y$	$\delta$ -effect in each loci
1	0 or 1	$Z_i * \Psi + \varepsilon_i$	$X_i\gamma + Z_i s + \epsilon_i$	None
2	0 or 1	$X_i * \alpha + Z_i * \Psi + \varepsilon_i$	$X_i\gamma + Z_i s + \epsilon_i$	None
3	0 or 1	$Z_i * \Psi + \varepsilon_i$	$Z_i s + \langle \mathbf{M}_i, \beta \rangle + \epsilon_i$	None
4	0 or 1	$X_i * \alpha + Z_i * \Psi + \varepsilon_i$	$Z_i s + \langle \mathbf{M}_i, \beta \rangle + \epsilon_i$	$\alpha \circ \beta$
5	0 or 1	$X_i * \alpha + Z_i * \Psi + \varepsilon_i$	$X_i\gamma + Z_i s + \langle \mathbf{M}_i, \beta \rangle + \epsilon_i$	$\alpha \circ \beta$

Here,  $\gamma = s = 10$ ,  $Z_i \sim \mathcal{U}(0, 2)$ ,  $X_i \sim \mathcal{B}(1, \pi_i)$ ,  $\text{logit}(\pi_i) = 0.5 - 0.5Z_i$ ,  $\text{vec}(\varepsilon_i) \sim \mathcal{N}(0, 0.2^2 I)$ ,  $\epsilon_i \sim \mathcal{N}(0, 0.1^2)$ .  $\Psi$ ,  $\alpha$  and  $\beta$  are shown in Figure S.1.

Each of the five scenarios has 100 replications. For each replication, the LISEMs are fitted using the approach outlined in Section 2. After estimation, a MaxP test (MacKinnon et al., 2002) based on the generated bootstrap sample is performed to determine which  $\alpha_{p_1, p_2, p_3} \beta_{p_1, p_2, p_3}$  is significantly different from 0. The results are controlled for multiple comparisons using the Benjamini-Hochberg procedure ( $q = 0.05$ ).

**Scenario 1** As shown in Table 1, the data are generated assuming  $\mathbf{M}_i = Z_i * \Psi + \epsilon_i$  and  $Y_i = X_i\gamma + Z_i s + \epsilon_i$  for  $i = 1, \dots, n$ , where  $\text{vec}(\epsilon_i) \sim \mathcal{N}(0, 0.2^2 I)$ ,  $\gamma = 10$ ,  $Z_i \sim \mathcal{U}(0, 2)$ ,  $X_i \sim \mathcal{B}(1, \pi_i)$ ,  $\text{logit}(\pi_i) = 0.5 - 0.5Z_i$ , and  $\epsilon_i \sim \mathcal{N}(0, 0.1^2)$ . In this scenario,  $X$  has a significant direct effect on  $Y$  but no indirect effect, that is,  $\gamma = 10$  and  $\alpha = \beta = \mathbf{0}$ . The estimate of  $\gamma$  is  $\hat{\gamma} = 9.9979$  and its confident interval is  $[9.9401, 10.0556]$ . The first two rows of Figure 1 show estimates of  $\alpha$ ,  $\beta$ , and  $\alpha \circ \beta$ , together with 95% bootstrap percentile confidence intervals of the corresponding straightened vectors. None of the effects appear to deviate significantly from 0 for all the loci. Figure 2(a) shows the proportion of times that  $\alpha \circ \beta$  is statistically significant (adjusted  $p \leq 0.05$ ) among the 100 replications for each locus. Clearly, the proportions for all loci fall well below 0.05, which shows that the estimation and testing for  $\alpha \circ \beta$  perform well.

**Scenario 2** The data are generated in an analogous manner as in Scenario 1, except that  $\mathbf{M}_i = X_i * \alpha + Z_i * \Psi + \epsilon_i$  for  $i = 1, \dots, n$ , where  $Z_i$ ,  $X_i$ , and  $\epsilon_i$  are defined as above. Again,  $X$  has a significant direct effect on  $Y$  but no indirect effect, that is,  $\gamma = 10$  and  $\beta = \mathbf{0}$ . Note that in this case,  $\alpha \neq \mathbf{0}$ , which is different from the setting of Scenario 1. The estimate of  $\gamma$  is  $\hat{\gamma} = 9.9476$  and its confident interval is  $[9.5989, 10.3381]$ . The third and fourth rows of Figure 1 show estimates of  $\alpha$ ,  $\beta$ , and  $\alpha \circ \beta$ , together with 95% bootstrap percentile confidence intervals of the corresponding straightened vectors. The estimates coincide with the true values, with only  $\alpha$  being significantly different from  $\mathbf{0}$  in the loci corresponding to the elements in  $\alpha$  which are nonzero. Figure 2(b) shows the proportion of times that  $\alpha \circ \beta$  is statistically significant (adjusted  $p \leq 0.05$ ) among the 100 replications for each locus. Again, all loci fall well below 0.05. Note that the proportion of false positives increases and approaches 0.05 in the loci corresponding to the elements in  $\alpha$  which are nonzero.

**Scenario 3** The data are generated assuming  $\mathbf{M}_i = Z_i * \Psi + \epsilon_i$  and  $Y_i = Z_i s + \langle \mathbf{M}_i, \beta \rangle + \epsilon_i$  for  $i = 1, \dots, n$ , where  $Z_i$  is defined as above, both  $\text{vec}(\epsilon_i)$  and  $\epsilon_i$  follow normal distributions as described before. In this scenario,  $X$  has no direct or indirect effect on  $Y$ , that is,  $\gamma = 0$  and  $\alpha = \mathbf{0}$ . The estimate of  $\gamma$  is  $\hat{\gamma} = -0.0016$  and its confidence interval is  $[-0.0494, 0.0466]$ . The fifth and sixth rows of Figure 1 show estimates of  $\alpha$ ,  $\beta$ , and  $\alpha \circ \beta$ , together with 95% bootstrap percentile confidence intervals of the corresponding straightened vectors. Again, the estimates coincide with the true values, with  $\beta$  being significantly different from  $\mathbf{0}$  in the loci corresponding to the elements that  $\beta$  are nonzero. Figure 2(c) shows the proportion of times that  $\alpha \circ \beta$  is statistically significant (adjusted  $p \leq 0.05$ ) among the 100 replications for each locus. Again, for all loci the proportion falls below 0.05.

**Scenario 4** The data are generated in an analogous manner as described in Scenario 3, except that  $\mathbf{M}_i = X_i * \alpha + Z_i * \Psi + \epsilon_i$  for  $i = 1, \dots, n$ , where  $Z_i$ ,  $X_i$ , and  $\text{vec}(\epsilon_i)$  are defined as above. In this scenario,  $X$  has an indirect effect on  $Y$  but no significant direct effect, and some loci in  $\mathbf{M}$

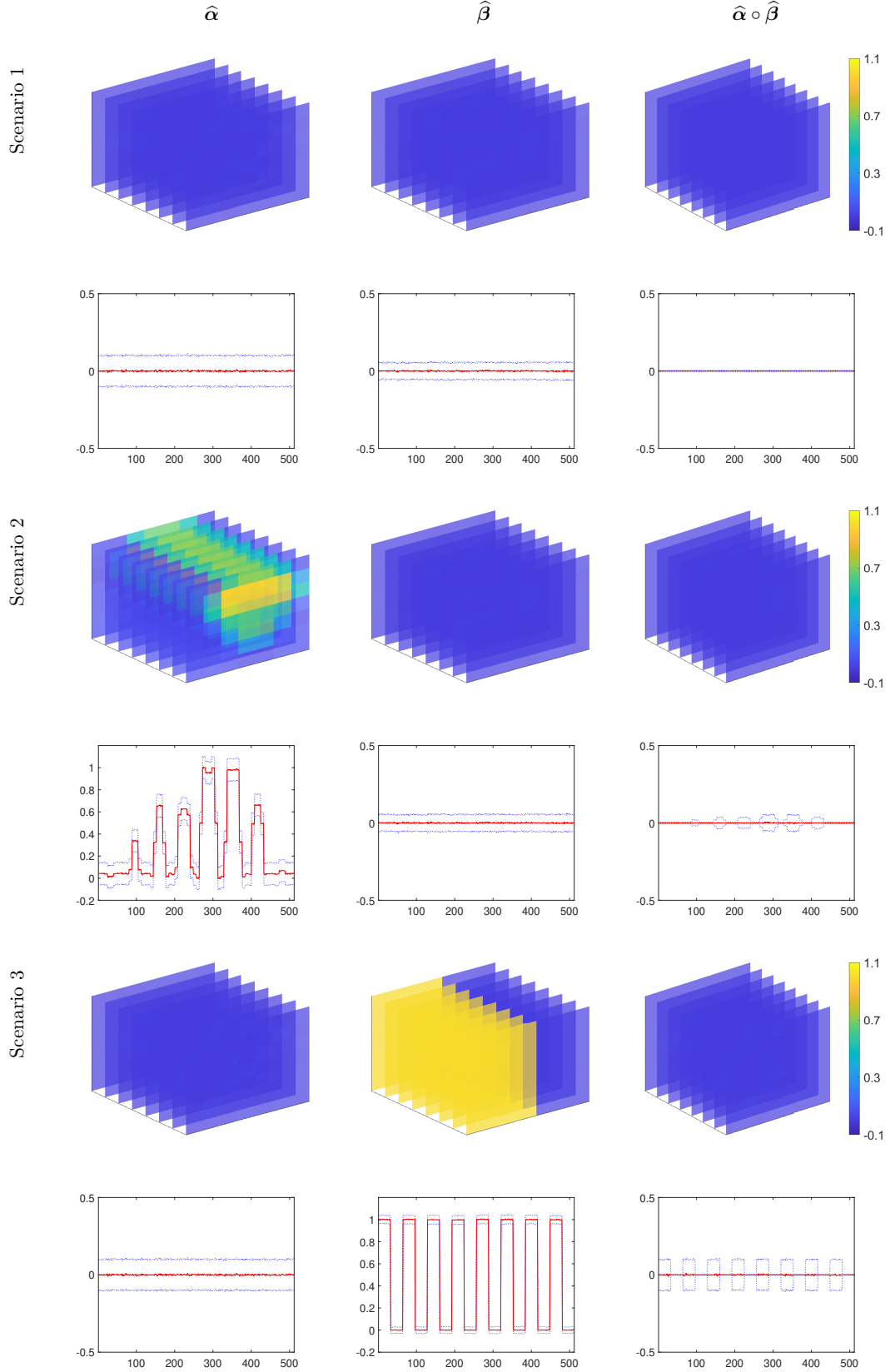


Figure 1: Estimates of  $\alpha$ ,  $\beta$ , and  $\alpha \circ \beta$ , together with 95% bootstrap percentile confidence intervals of the corresponding straightened vectors, for data generated according to the settings described in the Scenarios 1, 2, and 3. The  $x$ -axis of rows 2, 4 and 6 all represents the straightened loci, and the  $y$ -axis represents the values of the corresponding parameters at these loci. The colors in the images represent the grid point values.

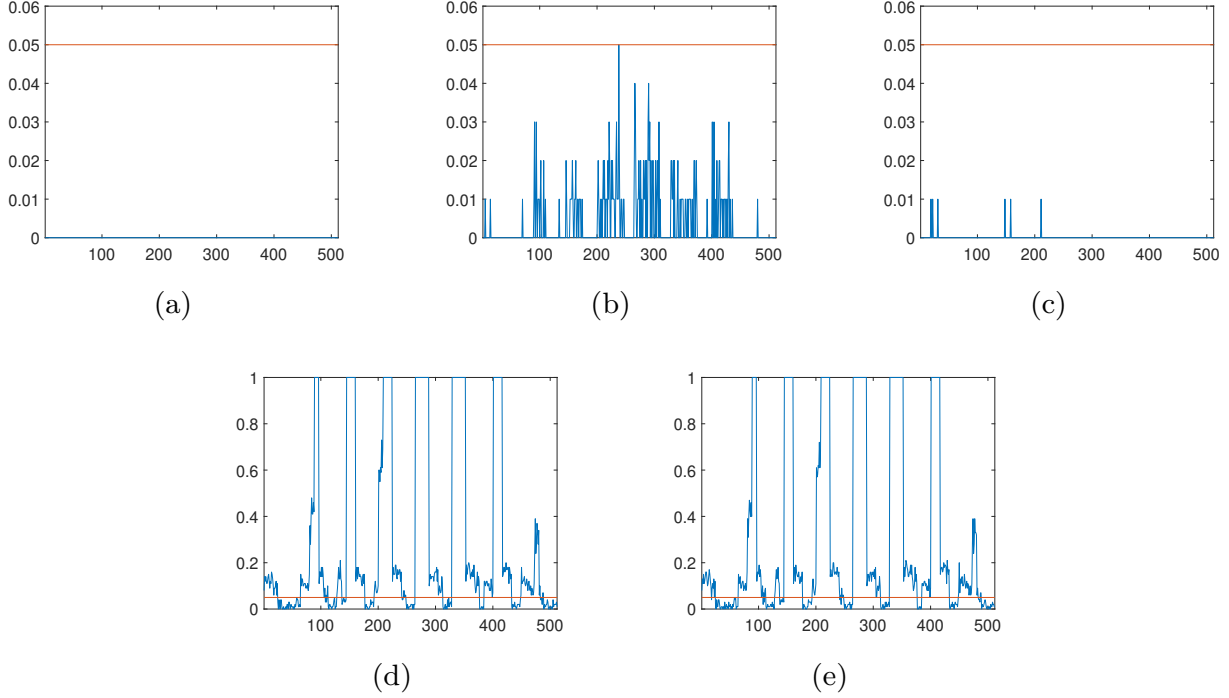


Figure 2: Results of the first three scenarios are shown in (a), (b), and (c), respectively. Each plot shows the proportion of times that  $\alpha \circ \beta$  is statistically significant (adjusted  $p < 0.05$ ) among the 100 replications for each locus. The results illustrate that the method provides adequate control of the false positive rate in all three simulated scenarios. Results of the last two scenarios are shown in (d) and (e), respectively. Each plot illustrates the power of the method in detecting true positives in the loci of  $\alpha_{p_1,p_2,p_3}\beta_{p_1,p_2,p_3} \neq 0$ , while appropriately controlling for false positives in the loci of  $\alpha_{p_1,p_2,p_3}\beta_{p_1,p_2,p_3} = 0$ . The  $x$ -axis of all plots represents the straightened loci.

transmit the effect of  $X$  on  $Y$ , that is,  $\gamma = 0$  and  $\alpha \circ \beta \neq \mathbf{0}$ . The estimate of  $\gamma$  is  $\hat{\gamma} = 0.0042$  and its confidence interval is  $[-0.5273, 0.5493]$ . The first two rows of Figure 3 show estimates of  $\alpha$ ,  $\beta$  and  $\alpha \circ \beta$ , together with 95% bootstrap percentile confidence intervals of the corresponding straightened vectors. Again, all three estimates coincide with the true values, as they are significantly different from 0 in the appropriate loci. Figure 2(d) illustrates the power of the method in detecting true positives in the loci where  $\alpha_{p_1,p_2,p_3}\beta_{p_1,p_2,p_3} \neq 0$ , while appropriately controlling for false positives in the loci where  $\alpha_{p_1,p_2,p_3}\beta_{p_1,p_2,p_3} = 0$ .

**Scenario 5** The data are generated in an analogous manner as described in Scenario 4, except that  $Y_i = X_i\gamma + Z_i s + \langle \mathbf{M}_i, \beta \rangle + \epsilon_i$  for  $i = 1, \dots, n$ , where  $\gamma = 10$ ,  $Z_i \sim \mathcal{U}(0, 2)$ ,  $\text{logit}(\pi_i) = 0.5 - 0.5Z_i$ ,  $X_i \sim \mathcal{B}(1, \pi_i)$ , and  $\epsilon_i \sim \mathcal{N}(0, 0.1^2)$ . In this scenario,  $X$  has both direct and indirect effect on  $Y$ , and some loci in  $\mathbf{M}$  transmit the effect of  $X$  on  $Y$ , that is,  $\gamma = 10$  and  $\alpha \circ \beta \neq \mathbf{0}$ . The estimate of  $\gamma$  is  $\hat{\gamma} = 10.0042$  and its confident interval is  $[9.4749, 10.5542]$ . The third and fourth rows of Figure 3 show estimates of  $\alpha$ ,  $\beta$  and  $\alpha \circ \beta$ , together with 95% bootstrap percentile confidence intervals of the corresponding straightened vectors. Similarly, all three estimates coincide with the true values, as they are significantly different from 0 in the appropriate loci. Figure 2(e) illustrates

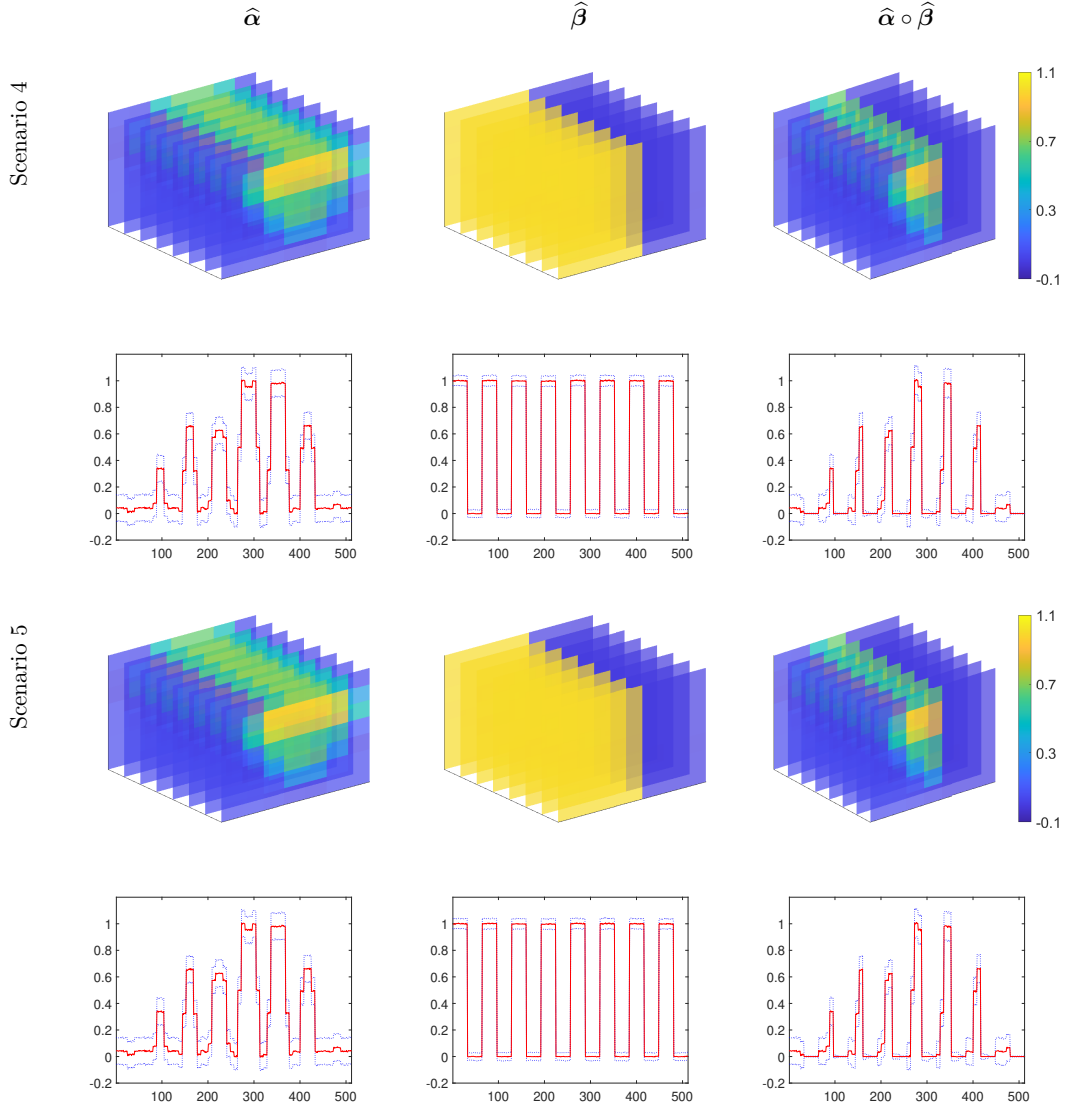


Figure 3: Estimates of  $\alpha$ ,  $\beta$ , and  $\alpha \circ \beta$ , together with 95% bootstrap percentile confidence intervals of the corresponding straightened vectors, for data generated according to the settings described in Scenarios 4 and 5. The  $x$ -axis represents the straightened loci, and the  $y$ -axis represents the values of the corresponding parameters at these loci. The colors in the images represent the grid point values.

the power of the method in detecting true positives in the intervals that  $\alpha_{p_1, p_2, p_3} \beta_{p_1, p_2, p_3} \neq 0$ , while appropriately controlling for false positives in the intervals that  $\alpha_{p_1, p_2, p_3} \beta_{p_1, p_2, p_3} = 0$ .

## 4 REAL DATA APPLICATION

Extensive scientific research have shown that the brain, as the carrier of human consciousness, profoundly affects the performance of human intelligence (e.g., [Reiss et al., 1996](#); [Haier et al., 2004](#); [Northam et al., 2011](#); [Liu et al., 2019](#)).

Recently, a systematic review and meta-analysis by [Zhang et al. \(2019\)](#) indicates that children

delivered through caesarean section are associated with an increased risk of negative performance in physical health and neurocognitive development, compared with children born via vaginal delivery. Blazkova et al. (2020) shows that children born with caesarean section score lower in psychological cognitive tests than those born via vaginal delivery. However, an earlier study (Li et al., 2011) on Chinese children finds no difference in intelligence quotient (IQ) scores between children who were delivered by caesarean section and spontaneous vaginal delivery. A more recent systematic review (Blake et al., 2021) concludes that the evidence of an association between caesarean section birth and lower offspring cognitive functioning is inconsistent.

Motivated by the controversial studies, this article considers two issues. The first is whether mother’s delivery mode has an impact on child’s intellectual performance, and the second is if this impact exists, whether it is mediated by the brain and which loci transmit the impact. These two issues can be tackled with the proposed ICMA method through estimating the causal parameters  $\alpha$ ,  $\gamma$ , and  $\beta$  in the LISEMs.

The real data are collected by the Institute of Brain Science, East China Normal University. The original dataset contains each child’s family status, physical and mental status, sleep duration and quality, parental characteristics, magnetic resonance brain images, and various test scores for 100 six-year-old children. Through prior studies that construct causal diagrams to explore relationship among variables (e.g., Andrews et al., 2018), eight variables are considered in the image casual mediation analysis, in which *delivery mode* is the treatment, *cerebrospinal fluid’s (CSF’s) MRI* or *gray matter’s MRI* or *white matter’s MRI* is the mediator, *child’s IQ score* is the outcome and *sex*, *maternal age*, *maternal education*, *oxytocin*, and *family type* are the pre-treatment covariates. Detailed description of these variables are shown in Table 2.

The ICMA method is applied to each of the three types of image mediators, respectively. Since the original image data is of dimension  $144 \times 192 \times 160$ , which is much larger than the sample size  $n = 93$ , directly applying the ICMA method to the original image data may cause computational difficulties and is often inefficient. Thus the real data study is divided into two parts.

In the first part, the original image is transformed into a  $9 \times 12 \times 10$  tensor via average pooling, that is, the value of each locus of the new tensor is the average value of the corresponding  $16 \times 16 \times 16$  cubic in the original image, see Figure S.3 for details. Then the ICMA method is applied to estimate the causal effects when the mediator is *CSF’s MRI* or *gray matter’s MRI* or *white matter’s MRI*, the results of these cases all show that caesarean section has statistically significant negative direct effect on child’s intellectual development (Table 3). Yet the indirect effects through the  $9 \times 12 \times 10$  tensors are all insignificant probably because there is much less information contained in the small tensor than the original image.

To further explore the indirect effect through the MRI, the second part selects some potential regions ( $16 \times 16 \times 16$  cubes) of the brain and applies the ICMA method with each region being

Table 2: Description of variables in real data analysis.

Variable		Name	Value	Sample size
Treatment	$X$	Delivery mode	1: Caesarean section 0: Spontaneous vaginal delivery	93
Mediator	$M$	CSF's MRI Gray matter's MRI White matter's MRI	$\mathcal{R}^{p_1 \times p_2 \times p_3}$	93
Outcome	$Y$	IQ score	$(0, \infty)$	93
Pre-treatment covariates	$Z_1$	Child's sex	1: Boy 0: Girl	93
	$Z_2$	Maternal age	$(0, \infty)$	93
	$Z_3$	Oxytocin	1: Yes 0: No	93
	$Z_{41}$	Family type-1	1: Family only consisting of children and their parents 0: Others	93
	$Z_{42}$	Family type-2	1: Family consisting of children, parents and grandparents 0: Others	93
	$Z_5$	Maternal education	$(0, \infty)$	93
Note:	<ol style="list-style-type: none"> <li>The MRIs here are all pre-processed, which are the output images of the raw MRIs after four steps' standardization processing by FSL Programs (bet2 (first step), FAST (third step)) and AFNI Programs (auto_warp.py (second step), 3dNwarpApply (fourth step)) based on the brain image in Figure S.2.</li> <li>The MRI data of each individual is divided into three classes based on CSF, Gray matter and White matter. The value of each locus in each class of image is the percentage of that class of tissue present at that locus.</li> </ol>			

Table 3: Results of the first part.

Tissue category	Direct effect $\gamma$	95% confidence interval of $\gamma$
CSF	-4.4201	(-0.4625,-8.3960)
Gray matter	-4.4265	(-0.4537,-8.4067)
White matter	-4.4145	(-4559,-8.3625)

an image mediator. Specifically, the regions with unadjusted  $p$ -value less than 0.2 in the first part of the analysis are selected as potential mediators. The results show that loci in some regions in the white matter have significant mediation effects after adjusting for  $p$ -values. The results are summarized in Table 4 and Figure 4.

A body of literature has detected the influences of the gray and white matter on the development of child's IQ (e.g., [Reiss et al., 1996](#); [Wilke et al., 2003](#); [Northam et al., 2011](#); [Isaacs et al., 2010](#);



Table 4: Results of the second part.

Tissue category	Number of the potential intermediary regions	Number of regions containing loci with significant indirect effects
CSF	86	0
Gray matter	59	0
White matter	44	7

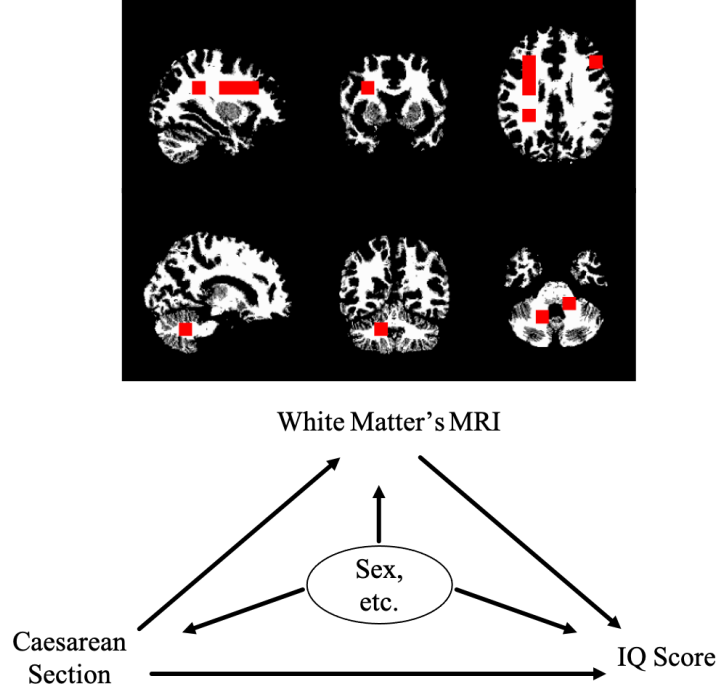


Figure 4: The causal diagram with the white matter’s MRI as the mediator. The first row of the image plot shows a slice map of the regions containing loci with statistically significant mediation effects in the frontal-parietal white matter via five red boxes (the percentage of loci with statistically significant mediation effects in each red box is in the range of 0.05%-20%). The second row shows a slice map of the regions containing loci with statistically significant mediation effects in the brainstem-cerebellum white matter via two red boxes (the percentage of loci with statistically significant mediation effects in each red box is about 0.61%).

Luby et al., 2016). Specifically, Luby et al. (2016) found the relationship between breastfeeding and childhood IQ is mediated by the gray matter volume. The results of our real data analysis indicate that caesarean section has a negative direct effect on child’s IQ when the *CSF’s MRI* (or *gray matter’s MRI* or *white matter’s MRI*) of the whole brain is considered as a mediator, and suggest that the white matter in the frontal-parietal and brainstem-cerebellum areas convey indirect effects from the caesarean section to child’s IQ development. These findings help address the controversial issues described earlier in this section. Additionally, since limited information is available surrounding the role of white matter in shaping cognitive abilities in children (Muetzel et al., 2015), our findings provide inspiration for future prospective and longitudinal studies.

## 5 Discussion

This article introduces the ICMA method to study image mediation effects. It defines the average casual effects under the potential outcome framework, examines sufficient conditions for the valid identification, and develops techniques for estimation and inference. Different from most brain mediation analysis literature that treat summary measures of brain regions as mediator, in this study the image data is directly modeled as the mediator, and pre-treatment covariates are considered.

Note that the LISEMs in this article assumes linearity. However, they can be easily extended to the generalized linear form, that is,

$$\begin{aligned}\mathcal{A}_1(\mu_{M|X=x, \mathbb{Z}=z}) &= \boldsymbol{\eta}_1 + x * \boldsymbol{\alpha} + \sum_{j=1}^J z_j * \boldsymbol{\Psi}_j, \\ \mathcal{A}_2(\mu_{Y|X=x, \mathbf{M}=\mathbf{m}, \mathbb{Z}=z}) &= \eta_2 + x\gamma + \langle \mathbf{m}, \boldsymbol{\beta} \rangle + \sum_{j=1}^J z_j s_j,\end{aligned}\tag{16}$$

where  $\mathcal{A}_1$  and  $\mathcal{A}_2$  are known link functions,  $\mu_{M|X=x, \mathbb{Z}=z} = E(\mathbf{M} | X = x, \mathbb{Z} = z)$ , and  $\mu_{Y|X=x, \mathbf{M}=\mathbf{m}, \mathbb{Z}=z} = E(Y | X = x, \mathbf{M} = \mathbf{m}, \mathbb{Z} = z)$ . In this formulation, under Assumption 2, the total effect  $\tau$  can be expressed as

$$\begin{aligned}\tau &= \gamma(x) + \delta(1 - x) \\ &= \int_{\mathbb{Z}} \int_{\mathcal{M}} \{E(Y | X = 1, \mathbf{M} = \mathbf{m}, \mathbb{Z} = z) - E(Y | X = 0, \mathbf{M} = \mathbf{m}, \mathbb{Z} = z)\} dF_{M|X=x, \mathbb{Z}=z}(\mathbf{m}) dF_{\mathbb{Z}}(z) \\ &\quad + \int_{\mathbb{Z}} \int_{\mathcal{M}} E(Y | X = 1 - x, \mathbf{M} = \mathbf{m}, \mathbb{Z} = z) \{dF_{M|X=1, \mathbb{Z}=z}(\mathbf{m}) - dF_{M|X=0, \mathbb{Z}=z}(\mathbf{m})\} dF_{\mathbb{Z}}(z) \\ &= \int_{\mathbb{Z}} \int_{\mathcal{M}} \{\mathcal{B}_2(\eta_2 + \gamma + \langle \mathbf{m}, \boldsymbol{\beta} \rangle + \sum_{j=1}^J z_j s_j) - \mathcal{B}_2(\eta_2 + \langle \mathbf{m}, \boldsymbol{\beta} \rangle + \sum_{j=1}^J z_j s_j)\} dF_{M|X=x, \mathbb{Z}=z}(\mathbf{m}) dF_{\mathbb{Z}}(z) \\ &\quad + \int_{\mathbb{Z}} \int_{\mathcal{M}} \mathcal{B}_2(\eta_2 + (1 - x)\gamma + \langle \mathbf{m}, \boldsymbol{\beta} \rangle + \sum_{j=1}^J z_j s_j) \{dF_{M|X=1, \mathbb{Z}=z}(\mathbf{m}) - dF_{M|X=0, \mathbb{Z}=z}(\mathbf{m})\} dF_{\mathbb{Z}}(z),\end{aligned}$$

where  $\mathcal{B}_2 = \mathcal{A}_2^{-1}$ . Specially, if  $\mathcal{B}_2$  is the identity function, then

$$\begin{aligned}\tau &= \int_{\mathbb{Z}} \int_{\mathcal{M}} \{\eta_2 + \gamma + \langle \mathbf{m}, \boldsymbol{\beta} \rangle + \sum_{j=1}^J z_j s_j - (\eta_2 + \langle \mathbf{m}, \boldsymbol{\beta} \rangle + \sum_{j=1}^J z_j s_j)\} dF_{M|X=x, \mathbb{Z}=z}(\mathbf{m}) dF_{\mathbb{Z}}(z) \\ &\quad + \int_{\mathbb{Z}} \int_{\mathcal{M}} (\eta_2 + (1 - x)\gamma + \langle \mathbf{m}, \boldsymbol{\beta} \rangle + \sum_{j=1}^J z_j s_j) \{dF_{M|X=1, \mathbb{Z}=z}(\mathbf{m}) - dF_{M|X=0, \mathbb{Z}=z}(\mathbf{m})\} dF_{\mathbb{Z}}(z) \\ &= \gamma + \int_{\mathbb{Z}} \langle \mathcal{B}_1(\boldsymbol{\eta}_1 + \boldsymbol{\alpha} + \sum_{j=1}^J z_j * \boldsymbol{\Psi}_j) - \mathcal{B}_1(\boldsymbol{\eta}_1 + \sum_{j=1}^J z_j * \boldsymbol{\Psi}_j), \boldsymbol{\beta} \rangle dF_{\mathbb{Z}}(z),\end{aligned}$$

where  $\mathcal{B}_1 = \mathcal{A}_1^{-1}$ . Obviously, when  $\mathcal{B}_1$  is also the identity function,  $\tau = \gamma + \langle \boldsymbol{\alpha}, \boldsymbol{\beta} \rangle$ .

In this study, only low-dimensional pre-treatment covariates are considered, high-dimensional cases such as the genetic data of children and their parents are not involved. Although there are some ways to deal with high-dimensional covariates (e.g., [Luo et al., 2017](#)), these methods may not be effective when the mediator is an image. A recent work ([Yu et al., 2022](#)) proposes a method to map the genetic-imaging-clinical pathway for Alzheimer’s disease, in which the treatment variable is a two-dimensional image, the covariates are ultra-high-dimensional clinical and genetic data, the outcome variable is a continuous scalar, and the relationship among them follow linear structural equation models. However, it is difficult to cope with a three-dimensional image mediator and high-dimensional covariates via this method, since the tensor nuclear norm is generally NP-hard to even approximate ([Friedland and Lim, 2018](#)). The problem of three-dimensional image mediator combined with high-dimensional covariates remains for future work. The post-treatment covariates are not considered here, since in many cases they are affected by treatment, which makes the identification of defined causal effects difficult. A possible solution is to define interventional effects ([VanderWeele et al., 2014](#)), and this issue is left for future work.

## APPENDIX A: PROOF OF IDENTIFICATION

### Proof of Theorem 1

Under Assumption 2 following the same argument of the Theorem 1 in [Imai et al. \(2010b\)](#), for  $x = 0, 1$ ,

$$\begin{aligned}\gamma(x) &= \int_{\mathbb{Z}} \int_{\mathcal{M}} \{E(Y \mid X = 1, \mathbf{M} = \mathbf{m}, \mathbb{Z} = z) \\ &\quad - E(Y \mid X = 0, \mathbf{M} = \mathbf{m}, \mathbb{Z} = z)\} dF_{\mathbf{M}|X=x, \mathbb{Z}=z}(\mathbf{m}) dF_{\mathbb{Z}}(z), \\ \delta(x) &= \int_{\mathbb{Z}} \int_{\mathcal{M}} E(Y \mid X = x, \mathbf{M} = \mathbf{m}, \mathbb{Z} = z) \\ &\quad \{dF_{\mathbf{M}|X=1, \mathbb{Z}=z}(\mathbf{m}) - dF_{\mathbf{M}|X=0, \mathbb{Z}=z}(\mathbf{m})\} dF_{\mathbb{Z}}(z),\end{aligned}$$

where  $F_{\mathbb{Z}}(\cdot)$  and  $F_{\mathbf{M}|X, \mathbb{Z}}(\cdot)$  represent the distribution function and the conditional distribution function.

Under Assumption 3,

$$\begin{aligned}
\gamma(x) &= \int_{\mathcal{Z}} \int_{\mathcal{M}} (\eta_2 + \gamma + \langle \mathbf{m}, \boldsymbol{\beta} \rangle + \sum_{j=1}^J z_j s_j - \eta_2 \\
&\quad - \langle \mathbf{m}, \boldsymbol{\beta} \rangle - \sum_{j=1}^J z_j s_j) dF_{\mathbf{M}|X=x, \mathbb{Z}=z}(\mathbf{m}) dF_{\mathbb{Z}}(z) \\
&= \gamma. \\
\delta(x) &= \int_{\mathcal{Z}} \int_{\mathcal{M}} (\eta_2 + x\gamma + \langle \mathbf{m}, \boldsymbol{\beta} \rangle + \sum_{j=1}^J z_j s_j) \\
&\quad \{dF_{\mathbf{M}|X=1, \mathbb{Z}=z}(\mathbf{m}) - dF_{\mathbf{M}|X=0, \mathbb{Z}=z}(\mathbf{m})\} dF_{\mathbb{Z}}(z) \\
&= \int_{\mathcal{Z}} (\langle E(\mathbf{M} | X = 1, \mathbb{Z} = z) - E(\mathbf{M} | X = 0, \mathbb{Z} = z), \boldsymbol{\beta} \rangle) dF_{\mathbb{Z}}(z) \\
&= \langle \boldsymbol{\alpha}, \boldsymbol{\beta} \rangle. \\
\tau &= \gamma(1) + \delta(0) = \gamma(0) + \delta(1) = \gamma + \langle \boldsymbol{\alpha}, \boldsymbol{\beta} \rangle.
\end{aligned}$$

## Proof of Lemma 1 and Theorem 2

**Lemma 1.** *Assumption 4 is weaker than Assumptions 2 and 3.*

First, note that Assumption 2 (a) implies

$$\begin{aligned}
\mathbf{M}_i(x) &\perp X_i | \mathbb{Z}_i = z & (*) \\
Y_i(x', \mathbf{m}) &\perp X_i | \mathbb{Z}_i = z & (**) \\
Y_i(x', \mathbf{m}) &\perp X_i | \mathbf{M}_i(x) = \mathbf{m}', \mathbb{Z}_i = z & (***)
\end{aligned}$$

According to (\*),  $E(\mathbf{M}(x) | X = x, \mathbb{Z} = z) = E(\mathbf{M}(x) | \mathbb{Z} = z)$ .

By (\*\*),

$$\begin{aligned}
&E(Y(x, \mathbf{M}(x)) | X = x, \mathbf{M}(x) = \mathbf{m}, \mathbb{Z} = z) \\
&= E(Y(x, \mathbf{m}) | X = x, \mathbf{M}(x) = \mathbf{m}, \mathbb{Z} = z) \\
&\stackrel{(***)}{=} E(Y(x, \mathbf{m}) | \mathbf{M}(x) = \mathbf{m}, \mathbb{Z} = z) \\
&= E(Y(x, \mathbf{M}(x)) | \mathbf{M}(x) = \mathbf{m}, \mathbb{Z} = z).
\end{aligned}$$

Then under Assumption 2 (b),  $(**)$  and  $(***)$ , we obtain

$$\begin{aligned}
& E(Y(x, \mathbf{M}(x)) \mid X = x', \mathbf{M}(x') = \mathbf{m}, \mathbb{Z} = z) \\
& \stackrel{2(b)}{=} E(Y(x, \mathbf{m}) \mid X = x', \mathbb{Z} = z) \\
& \stackrel{(**)}{=} E(Y(x, \mathbf{m}) \mid \mathbb{Z} = z), \\
& E(Y(x, \mathbf{m}) \mid X = x', \mathbf{M}(x') = \mathbf{m}, \mathbb{Z} = z) \\
& \stackrel{(***)}{=} E(Y(x, \mathbf{m}) \mid \mathbf{M}(x') = \mathbf{m}, \mathbb{Z} = z), \\
& E(Y(x, \mathbf{m}) \mid \mathbf{M}(x') = \mathbf{m}, \mathbb{Z} = z) = E(Y(x, \mathbf{m}) \mid \mathbb{Z} = z).
\end{aligned}$$

Additionally, obviously, Assumption 4 (c) can be deduced by  $0 < \Pr(X = x \mid \mathbb{Z}_i = z)$  and  $0 < p(\mathbf{M}(x) = \mathbf{m} \mid X = x, \mathbb{Z} = z)$ .

Further, under Assumption 2,

$$\begin{aligned}
& E(\mathbf{M}(x) \mid \mathbb{Z} = z) \\
& = E(\mathbf{M}(x) \mid X = x, \mathbb{Z} = z) \\
& = E(\mathbf{M} \mid X = x, \mathbb{Z} = z), \\
& E(Y(x, \mathbf{m}) \mid \mathbb{Z} = z) \\
& = E(Y(x, \mathbf{m}) \mid X = x, \mathbb{Z} = z) \\
& = \int_{\mathcal{M}} E(Y(x, \mathbf{m})) \mid X = x, \mathbf{M}(x) = \mathbf{m}, \mathbb{Z} = z) dF_{\mathbf{M}(x) \mid X=x, \mathbb{Z}=z}(\mathbf{m}) \\
& = \int_{\mathcal{M}} E(Y \mid X = x, \mathbf{M}(x) = \mathbf{m}, \mathbb{Z} = z) dF_{\mathbf{M} \mid X=x, \mathbb{Z}=z}(\mathbf{m}).
\end{aligned}$$

Then by Assumption 3,

$$\begin{aligned}
E(\mathbf{M}(x) \mid \mathbb{Z} = z) &= \boldsymbol{\eta}_1 + x * \boldsymbol{\alpha} + \sum_{j=1}^J z_j * \boldsymbol{\Psi}_j, \\
E(Y(x, \mathbf{m}) \mid \mathbb{Z} = z) &= \eta_2 + x\gamma + \langle \mathbf{m}, \boldsymbol{\beta} \rangle + \sum_{j=1}^J z_j s_j.
\end{aligned}$$

Thus, Assumptions 2 and 3 imply Assumption 4. However, in general, the mean independence between two random variables does not imply they are independent of each other. Thus the inverse does not hold. Hence, Assumption 4 is weaker than Assumptions 2 and 3.

Next, we prove Theorem 2.

Under Assumptions 1 and 4,

$$\begin{aligned}
E(\mathbf{M} \mid X = x, \mathbb{Z} = z) &= E(\mathbf{M}(X) \mid X = x, \mathbb{Z} = z) \\
&= E(\mathbf{M}(x) \mid X = x, \mathbb{Z} = z) \\
&= E(\mathbf{M}(x) \mid \mathbb{Z} = z) \\
&= \boldsymbol{\eta}_1^{(c)} + x * \boldsymbol{\alpha}^{(c)} + \sum_{j=1}^J z_j * \boldsymbol{\Psi}_j^{(c)}. \\
E(Y \mid X = x, \mathbf{M}(X) = \mathbf{m}, \mathbb{Z} = z) &= E(Y(X, \mathbf{M}(X)) \mid X = x, \mathbf{M}(X) = \mathbf{m}, \mathbb{Z} = z) \\
&= E(Y(x, \mathbf{M}(x)) \mid X = x, \mathbf{M}(x) = \mathbf{m}, \mathbb{Z} = z) \\
&= E(Y(x, \mathbf{M}(x)) \mid \mathbf{M}(x) = \mathbf{m}, \mathbb{Z} = z) \\
&= E(Y(x, \mathbf{m}) \mid \mathbf{M}(x) = \mathbf{m}, \mathbb{Z} = z) \\
&= E(Y(x, \mathbf{m}) \mid \mathbb{Z} = z) \\
&= \eta_2^{(c)} + x\gamma^{(c)} + \langle \mathbf{m}, \boldsymbol{\beta}^{(c)} \rangle + \sum_{j=1}^J z_j s_j^{(c)}.
\end{aligned}$$

Comparing the results above with the LISEMs, then

$$\begin{aligned}
(\boldsymbol{\eta}_1^{(c)} - \boldsymbol{\eta}_1) + x * (\boldsymbol{\alpha}^{(c)} - \boldsymbol{\alpha}) + \sum_{j=1}^J z_j * (\boldsymbol{\Psi}_j^{(c)} - \boldsymbol{\Psi}) &= \mathbf{0}, \\
(\eta_2^{(c)} - \eta_2) + x(\gamma^{(c)} - \gamma) + \langle \mathbf{m}, \boldsymbol{\beta}^{(c)} - \boldsymbol{\beta} \rangle + \sum_{j=1}^J z_j(s_j^{(c)} - s_j) &= 0.
\end{aligned}$$

Since  $x, \mathbf{m}, z$  are arbitrary, then  $\boldsymbol{\alpha}^{(c)} = \boldsymbol{\alpha}$ ,  $\gamma^{(c)} = \gamma$ ,  $\boldsymbol{\beta}^{(c)} = \boldsymbol{\beta}$ . This follows that  $E(\mathbf{M}(1) - \mathbf{M}(0)) = \boldsymbol{\alpha}$ ,  $E(Y(1, \mathbf{m}) - Y(0, \mathbf{m})) = \gamma$  and  $E(Y(x, \mathbf{m}) - Y(x, \mathbf{m}')) = \langle \mathbf{m} - \mathbf{m}', \boldsymbol{\beta} \rangle$ .

Further, under Assumptions 1 and 4,

$$\begin{aligned}
E(Y(x, \mathbf{M}(x')) \mid \mathbb{Z} = z) &= \int_{\mathcal{M}} E(Y(x, \mathbf{M}(x')) \mid \mathbf{M}(x') = \mathbf{m}, \mathbb{Z} = z) dF_{\mathbf{M}(x') \mid \mathbb{Z}=z}(\mathbf{m}) \\
&= \int_{\mathcal{M}} E(Y(x, \mathbf{m}) \mid \mathbf{M}(x') = \mathbf{m}, \mathbb{Z} = z) dF_{\mathbf{M}(x') \mid \mathbb{Z}=z}(\mathbf{m}) \\
&= \int_{\mathcal{M}} E(Y(x, \mathbf{m}) \mid \mathbb{Z} = z) dF_{\mathbf{M}(x') \mid \mathbb{Z}=z}(\mathbf{m}) \\
&= \int_{\mathcal{M}} (\eta_2^{(c)} + x\gamma^{(c)} + \langle \mathbf{m}, \boldsymbol{\beta}^{(c)} \rangle + \sum_{j=1}^J z_j s_j^{(c)}) dF_{\mathbf{M}(x') \mid \mathbb{Z}=z}(\mathbf{m}) \\
&= \eta_2^{(c)} + x\gamma^{(c)} + \langle E(\mathbf{M}(x') \mid \mathbb{Z} = z), \boldsymbol{\beta}^{(c)} \rangle + \sum_{j=1}^J z_j s_j \\
&= \eta_2^{(c)} + x\gamma^{(c)} + \langle \boldsymbol{\eta}_1^{(c)} + x' * \boldsymbol{\alpha}^{(c)} + \sum_{j=1}^J z_j * \boldsymbol{\Psi}_j^{(c)}, \boldsymbol{\beta}^{(c)} \rangle + \sum_{j=1}^J z_j s_j^{(c)} \\
&= \eta_2^{(c)} + \langle \boldsymbol{\eta}_1^{(c)}, \boldsymbol{\beta}^{(c)} \rangle + x\gamma^{(c)} + x' \langle \boldsymbol{\alpha}^{(c)}, \boldsymbol{\beta}^{(c)} \rangle + \sum_{j=1}^J z_j \left( \langle \boldsymbol{\Psi}_j^{(c)}, \boldsymbol{\beta}^{(c)} \rangle + s_j^{(c)} \right).
\end{aligned}$$

Hence,  $\tau = \gamma + \langle \boldsymbol{\beta}, \boldsymbol{\alpha} \rangle$ ,  $\gamma(x) = \gamma$ ,  $\delta(x) = \langle \boldsymbol{\beta}, \boldsymbol{\alpha} \rangle$ .

## APPENDIX B: PROOF OF THE PROPOSITION 1

Let,  $U \otimes V$  denotes Kronecker product between  $U$  and  $V$ . Since  $\widehat{\Delta} = (A_{X,Z}^T A_{X,Z})^{-1} A_{X,Z}^T M$ , then  $\widehat{\varepsilon} = (I - A_{X,Z} (A_{X,Z}^T A_{X,Z})^{-1} A_{X,Z}^T) \varepsilon$ .

Due to  $A_{X,Z} = B_{X,Z} \otimes I$ ,  $\varepsilon = \text{vec}(A_\varepsilon^T)$ ,  $\widehat{\varepsilon} = \text{vec}(A_{\widehat{\varepsilon}}^T)$  and the Properties of Kronecker product, then  $\text{vec}(A_{\widehat{\varepsilon}}^T) = (I - (B_{X,Z} \otimes I)((B_{X,Z} \otimes I)^T (B_{X,Z} \otimes I))^{-1} (B_{X,Z}^T \otimes I)) \text{vec}(A_\varepsilon^T) = ((I - B_{X,Z} (B_{X,Z}^T B_{X,Z})^{-1} B_{X,Z}^T) \otimes I) \text{vec}(A_\varepsilon^T)$ , that is,  $\text{vec}(A_{\widehat{\varepsilon}}^T) = \text{vec}(A_\varepsilon^T (I - B_{X,Z} (B_{X,Z}^T B_{X,Z})^{-1} B_{X,Z}^T))$ . Thus,  $A_{\widehat{\varepsilon}} = (I - B_{X,Z} (B_{X,Z}^T B_{X,Z})^{-1} B_{X,Z}^T) A_\varepsilon$ .

Therefore,

$$\begin{aligned}
\widehat{\omega} &= Y - B_{X,Z} \widehat{\Theta} \\
&= (I - B_{X,Z} (B_{X,Z}^T B_{X,Z})^{-1} B_{X,Z}^T) A_\varepsilon \beta + (I - B_{X,Z} (B_{X,Z}^T B_{X,Z})^{-1} B_{X,Z}^T) \epsilon \\
&= A_{\widehat{\varepsilon}} \beta + \widehat{\epsilon}.
\end{aligned}$$

## APPENDIX C: SUPPLEMENTARY FIGURES FOR SIMULATION STUDIES AND REAL DATA ANALYSIS

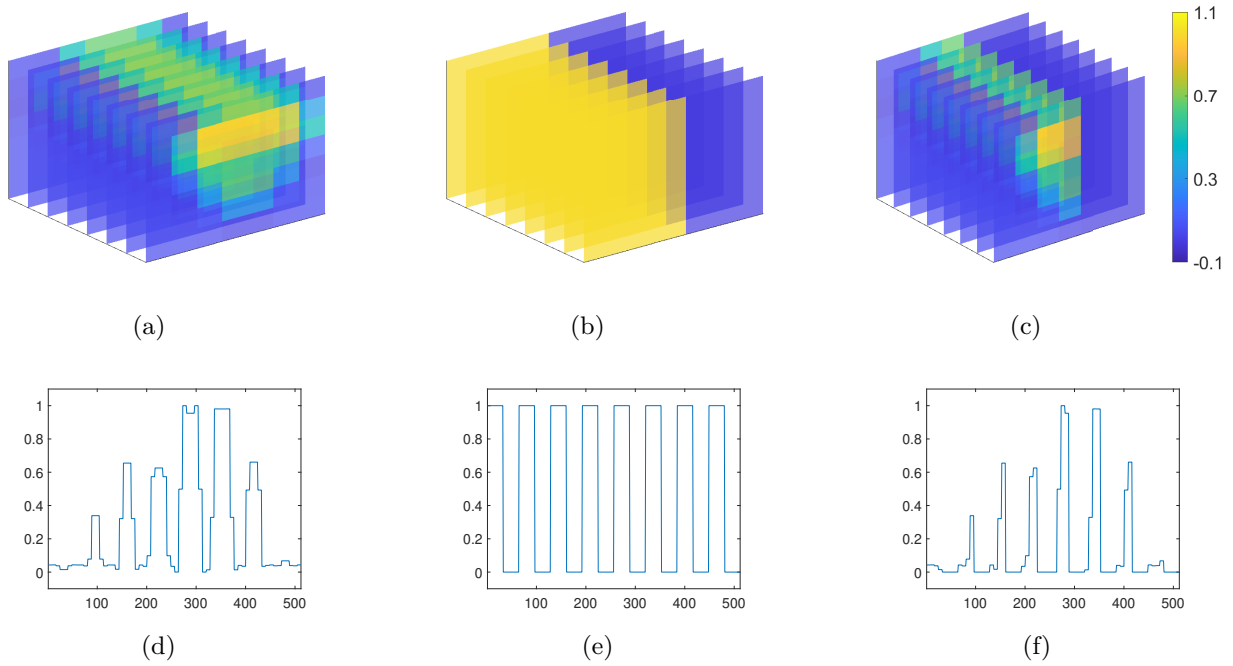


Figure S.1: (a) represents the slice image of  $\alpha$  and  $\Psi$ , and the non-zero part of it is a mixed-color elliptical cylinder. (b) represents the slice image of  $\beta$ , which is generated by two cubes of different colors. (c) represents the slice image of  $\alpha\beta$ . The colors represent the grid point values. (d) represents the plots of  $\text{vec}(\alpha)$  or  $\text{vec}(\Psi)$ , and (e), (f) represent the plots of  $\text{vec}(\beta)$  and  $\text{vec}(\alpha\beta)$ .

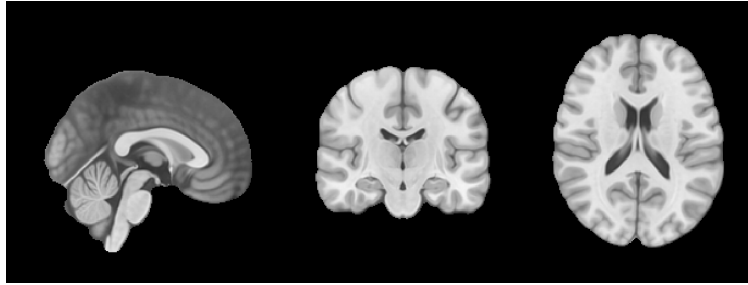


Figure S.2: The MNI152 standard-space T1-weighted average structural template image.

## ACKNOWLEDGMENTS

This work was supported by the National Natural Science Foundation of China (No.11771146, No.11831008), the Basic Research Project of Shanghai Science and Technology Commission (No.19JC1410101), and the “Flower of Happiness” Fund Pilot Project of East China Normal University (No.2019JK2203).

## DATA AVAILABILITY STATEMENT

The data supporting the findings of this study can be obtained by application to the Institute of Brain Science, East China Normal University. The data are not publicly available due to privacy or ethics or restrictions.



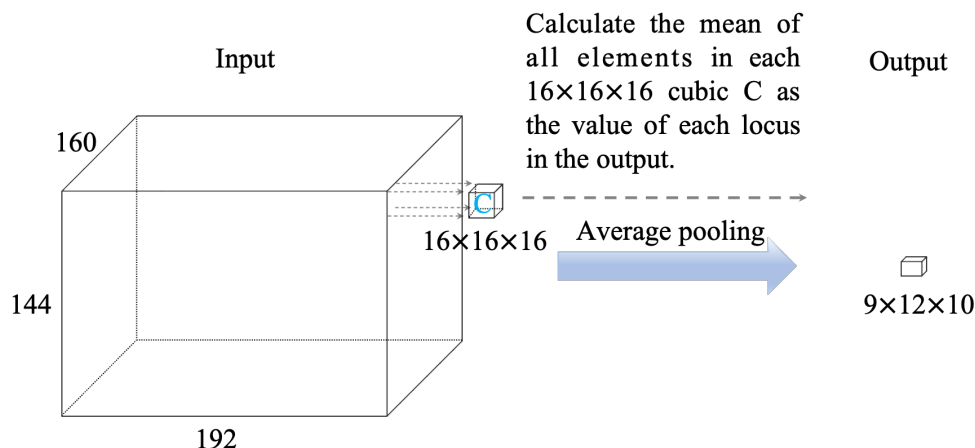


Figure S.3: Average pooling.

## REFERENCES

- Ahmed, T., Raja, H., and Bajwa, W. U. (2020). Tensor regression using low-rank and sparse tucker decompositions. *SIAM Journal on Mathematics of Data Science*, 2(4):944–966.
- Albert, J. M. (2008). Mediation analysis via potential outcomes models. *Statistics in medicine*, 27(8):1282–1304.
- Andrews, B., Ramsey, J., and Cooper, G. F. (2018). Scoring bayesian networks of mixed variables. *International journal of data science and analytics*, 6(1):3–18.
- Angrist, J. D., Imbens, G. W., and Rubin, D. B. (1996). Identification of causal effects using instrumental variables. *Journal of the American statistical Association*, 91(434):444–455.
- Avin, C., Shpitser, I., and Pearl, J. (2005). Identifiability of path-specific effects. In *Proceedings of the 19th international joint conference on Artificial intelligence*, pages 357–363. Morgan Kaufman, San Francisco, CA.
- Baron, R. M. and Kenny, D. A. (1986). The moderator–mediator variable distinction in social psychological research: Conceptual, strategic, and statistical considerations. *Journal of personality and social psychology*, 51(6):1173.
- Benjamini, Y. and Hochberg, Y. (1995). Controlling the false discovery rate: a practical and powerful approach to multiple testing. *Journal of the Royal statistical society: series B (Methodological)*, 57(1):289–300.
- Blake, J. A., Gardner, M., Najman, J., and Scott, J. G. (2021). The association of birth by caesarean section and cognitive outcomes in offspring: a systematic review. *Social Psychiatry and Psychiatric Epidemiology*, 56(4):533–545.

- Blazkova, B., Pastorkova, A., Solansky, I., Veleminsky, M., Rossnerova, A., Honkova, K., Rossner, P., and Sram, R. J. (2020). The impact of cesarean and vaginal delivery on results of psychological cognitive test in 5 year old children. *Medicina*, 56(10):554.
- Caffo, B., Chen, S., Stewart, W., Bolla, K., Yousem, D., Davatzikos, C., and Schwartz, B. S. (2008). Are brain volumes based on magnetic resonance imaging mediators of the associations of cumulative lead dose with cognitive function? *American journal of epidemiology*, 167(4):429–437.
- Casey, B., Tottenham, N., Liston, C., and Durston, S. (2005). Imaging the developing brain: what have we learned about cognitive development? *Trends in cognitive sciences*, 9(3):104–110.
- Dai, J. Y., Stanford, J. L., and LeBlanc, M. (2020). A multiple-testing procedure for high-dimensional mediation hypotheses. *Journal of the American Statistical Association*, pages 1–16.
- Daniel, R. M., De Stavola, B. L., Cousens, S., and Vansteelandt, S. (2015). Causal mediation analysis with multiple mediators. *Biometrics*, 71(1):1–14.
- De Lathauwer, L., De Moor, B., and Vandewalle, J. (2000). A multilinear singular value decomposition. *SIAM journal on Matrix Analysis and Applications*, 21(4):1253–1278.
- Derkach, A., Pfeiffer, R. M., Chen, T.-H., and Sampson, J. N. (2019). High dimensional mediation analysis with latent variables. *Biometrics*, 75(3):745–756.
- Efron, B. and Tibshirani, R. J. (1994). *An introduction to the bootstrap*. CRC press.
- Flachaire, E. (2005). Bootstrapping heteroskedastic regression models: wild bootstrap vs. pairs bootstrap. *Computational Statistics & Data Analysis*, 49(2):361–376.
- Friedland, S. and Lim, L.-H. (2018). Nuclear norm of higher-order tensors. *Mathematics of Computation*, 87(311):1255–1281.
- Giedd, J. N. and Rapoport, J. L. (2010). Structural mri of pediatric brain development: what have we learned and where are we going? *Neuron*, 67(5):728–734.
- Guo, X., Li, R., Liu, J., and Zeng, M. (2022). Statistical inference for linear mediation models with high-dimensional mediators and application to studying stock reaction to covid-19 pandemic. *Journal of Econometrics*.
- Haier, R. J., Jung, R. E., Yeo, R. A., Head, K., and Alkire, M. T. (2004). Structural brain variation and general intelligence. *Neuroimage*, 23(1):425–433.
- Han, R., Willett, R., and Zhang, A. R. (2022). An optimal statistical and computational framework for generalized tensor estimation. *The Annals of Statistics*, 50(1):1–29.
- Hoff, P. D. (2011). Separable covariance arrays via the tucker product, with applications to multi-variate relational data. *Bayesian Analysis*, 6(2):179–196.

- Imai, K., Keele, L., and Tingley, D. (2010a). A general approach to causal mediation analysis. *Psychological methods*, 15(4):309.
- Imai, K., Keele, L., and Yamamoto, T. (2010b). Identification, inference and sensitivity analysis for causal mediation effects. *Statistical science*, 25(1):51–71.
- Isaacs, E. B., Fischl, B. R., Quinn, B. T., Chong, W. K., Gadian, D. G., and Lucas, A. (2010). Impact of breast milk on intelligence quotient, brain size, and white matter development. *Pediatric research*, 67(4):357–362.
- James, L. R. and Brett, J. M. (1984). Mediators, moderators, and tests for mediation. *Journal of applied psychology*, 69(2):307.
- Kressner, D. and Perisa, L. (2017). Recompression of hadamard products of tensors in tucker format. *SIAM Journal on Scientific Computing*, 39(5):A1879–A1902.
- Li, C. (2011). *Compressive sensing for 3D data processing tasks: applications, models and algorithms*. Rice University.
- Li, H.-T., Ye, R.-W., Pei, L.-J., Ren, A.-G., Zheng, X.-Y., and Liu, J.-M. (2011). Cesarean delivery on maternal request and childhood intelligence: a cohort study.
- Lindquist, M. A. (2012). Functional causal mediation analysis with an application to brain connectivity. *Journal of the American Statistical Association*, 107(500):1297–1309.
- Liu, Y., Schubert, J., Sonnenberg, L., Helbig, K. L., Hoei-Hansen, C. E., Koko, M., Rannap, M., Lauxmann, S., Huq, M., Schneider, M. C., et al. (2019). Neuronal mechanisms of mutations in *scn8a* causing epilepsy or intellectual disability. *Brain*, 142(2):376–390.
- Liu, Z., Shen, J., Barfield, R., Schwartz, J., Baccarelli, A. A., and Lin, X. (2022). Large-scale hypothesis testing for causal mediation effects with applications in genome-wide epigenetic studies. *Journal of the American Statistical Association*, 117(537):67–81.
- Luby, J. L., Belden, A. C., Whalen, D., Harms, M. P., and Barch, D. M. (2016). Breastfeeding and childhood iq: The mediating role of gray matter volume. *Journal of the American Academy of Child & Adolescent Psychiatry*, 55(5):367–375.
- Luo, W., Zhu, Y., and Ghosh, D. (2017). On estimating regression-based causal effects using sufficient dimension reduction. *Biometrika*, 104(1):51–65.
- Luo, Y. and Zhang, A. R. (2021). Low-rank tensor estimation via riemannian gauss-newton: Statistical optimality and second-order convergence. *arXiv preprint arXiv:2104.12031*.
- MacKinnon, D. P., Lockwood, C. M., Hoffman, J. M., West, S. G., and Sheets, V. (2002). A comparison of methods to test mediation and other intervening variable effects. *Psychological methods*, 7(1):83.

- Miles, C. H., Shpitser, I., Kanki, P., Meloni, S., and Tchetgen Tchetgen, E. J. (2020). On semi-parametric estimation of a path-specific effect in the presence of mediator-outcome confounding. *Biometrika*, 107(1):159–172.
- Muetzel, R. L., Mous, S. E., van der Ende, J., Blanken, L. M., van der Lugt, A., Jaddoe, V. W., Verhulst, F. C., Tiemeier, H., and White, T. (2015). White matter integrity and cognitive performance in school-age children: a population-based neuroimaging study. *Neuroimage*, 119:119–128.
- Northam, G. B., Liégeois, F., Chong, W. K., S. Wyatt, J., and Baldeweg, T. (2011). Total brain white matter is a major determinant of iq in adolescents born preterm. *Annals of neurology*, 69(4):702–711.
- Pearl, J. (2001). Direct and indirect effects. In *Proceedings of the Seventeenth conference on Uncertainty in artificial intelligence* (J. S. Breese and D. Koller, eds.), pages 411–420. Morgan Kaufman, San Francisco, CA.
- Petersen, M. L., Sinisi, S. E., and van der Laan, M. J. (2006). Estimation of direct causal effects. *Epidemiology*, pages 276–284.
- Rauhut, H., Schneider, R., and Stojanac, Ž. (2017). Low rank tensor recovery via iterative hard thresholding. *Linear Algebra and its Applications*, 523:220–262.
- Reiss, A. L., Abrams, M. T., Singer, H. S., Ross, J. L., and Denckla, M. B. (1996). Brain development, gender and iq in children: a volumetric imaging study. *Brain*, 119(5):1763–1774.
- Robins, J. M. (2003). Semantics of causal dag models and the identification of direct and indirect effects. *Oxford Statistical Science Series*, pages 70–82.
- Robins, J. M. and Greenland, S. (1992). Identifiability and exchangeability for direct and indirect effects. *Epidemiology*, pages 143–155.
- Rubin, D. B. (1974). Estimating causal effects of treatments in randomized and nonrandomized studies. *Journal of educational Psychology*, 66(5):688.
- Rubin, D. B. (1980). Randomization analysis of experimental data: The fisher randomization test comment. *Journal of the American Statistical Association*, 75(371):591–593.
- Rubin, D. B. (2004). Direct and indirect causal effects via potential outcomes. *Scandinavian Journal of Statistics*, 31(2):161–170.
- Sobel, M. E. (1982). Asymptotic confidence intervals for indirect effects in structural equation models. *Sociological methodology*, 13:290–312.
- Sobel, M. E. (2008). Identification of causal parameters in randomized studies with mediating variables. *Journal of Educational and Behavioral Statistics*, 33(2):230–251.

- Tibshirani, R. (1996). Regression shrinkage and selection via the lasso. *Journal of the Royal Statistical Society: Series B (Methodological)*, 58(1):267–288.
- Tucker, L. R. (1966). Some mathematical notes on three-mode factor analysis. *Psychometrika*, 31(3):279–311.
- Van de Geer, S., Bühlmann, P., Ritov, Y., and Dezeure, R. (2014). On asymptotically optimal confidence regions and tests for high-dimensional models. *The Annals of Statistics*, 42(3):1166–1202.
- VanderWeele, T. (2015). *Explanation in causal inference: methods for mediation and interaction*. Oxford University Press.
- VanderWeele, T. and Vansteelandt, S. (2014). Mediation analysis with multiple mediators. *Epidemiologic methods*, 2(1):95–115.
- VanderWeele, T. J., Vansteelandt, S., and Robins, J. M. (2014). Effect decomposition in the presence of an exposure-induced mediator-outcome confounder. *Epidemiology (Cambridge, Mass.)*, 25(2):300.
- Wang, X., Zhu, H., and Initiative, A. D. N. (2017). Generalized scalar-on-image regression models via total variation. *Journal of the American Statistical Association*, 112(519):1156–1168.
- Wilke, M., Sohn, J.-H., Byars, A. W., and Holland, S. K. (2003). Bright spots: correlations of gray matter volume with iq in a normal pediatric population. *Neuroimage*, 20(1):202–215.
- Yu, D., Wang, L., Kong, D., and Zhu, H. (2022). Mapping the genetic-imaging-clinical pathway with applications to alzheimer’s disease. *Journal of the American Statistical Association*, (just-accepted):1–30.
- Zhang, C.-H. and Zhang, S. S. (2014). Confidence intervals for low dimensional parameters in high dimensional linear models. *Journal of the Royal Statistical Society: Series B (Statistical Methodology)*, 76(1):217–242.
- Zhang, H., Zheng, Y., Hou, L., Zheng, C., and Liu, L. (2021). Mediation analysis for survival data with high-dimensional mediators. *Bioinformatics*, 37(21):3815–3821.
- Zhang, T., Sidorchuk, A., Sevilla-Cermeño, L., Vilaplana-Pérez, A., Chang, Z., Larsson, H., Mataix-Cols, D., and de la Cruz, L. F. (2019). Association of cesarean delivery with risk of neurodevelopmental and psychiatric disorders in the offspring: a systematic review and meta-analysis. *JAMA network open*, 2(8):e1910236–e1910236.
- Zhang, Y., Shao, J., Yu, M., and Wang, L. (2018). Impact of sufficient dimension reduction in nonparametric estimation of causal effect. *Statistical Theory and Related Fields*, 2(1):89–95.

- Zhang, Y., Wang, L., Yu, M., and Shao, J. (2020). Quantile treatment effect estimation with dimension reduction. *Statistical Theory and Related Fields*, 4(2):202–213.
- Zhao, Y., Li, L., and Caffo, B. S. (2021). Multimodal neuroimaging data integration and pathway analysis. *Biometrics*, 77(3):879–889.
- Zhao, Y. and Luo, X. (2019). Granger mediation analysis of multiple time series with an application to functional magnetic resonance imaging. *Biometrics*, 75(3):788–798.
- Zheng, C. and Zhou, X.-H. (2015). Causal mediation analysis in the multilevel intervention and multicomponent mediator case. *Journal of the Royal Statistical Society: Series B (Statistical Methodology)*, 77(3):581–615.
- Zhou, H. and Li, L. (2014). Regularized matrix regression. *Journal of the Royal Statistical Society: Series B (Statistical Methodology)*, 76(2):463–483.
- Zhou, H., Li, L., and Zhu, H. (2013). Tensor regression with applications in neuroimaging data analysis. *Journal of the American Statistical Association*, 108(502):540–552.
- Zhou, R. R., Wang, L., and Zhao, S. D. (2020). Estimation and inference for the indirect effect in high-dimensional linear mediation models. *Biometrika*, 107(3):573–589.
- Zhu, H., Ibrahim, J. G., Tang, N., Rowe, D. B., Hao, X., Bansal, R., and Peterson, B. S. (2007). A statistical analysis of brain morphology using wild bootstrapping. *IEEE Transactions on Medical Imaging*, 26(7):954–966.